RESEARCH ARTICLE

water
ENVIRONMENT RESEARCH

Green production of hydrochar nut group from waste materials in subcritical water medium and investigation of their adsorption performance for crystal violet

Mohammed Saleh[1] | Zelal Isik[1] | Erdal Yabalak[2] (ID) | Mutlu Yalvac[1] |
Nadir Dizge[1] (ID)

[1]Department of Environmental
Engineering, Mersin University, Mersin,
Turkey

[2]Department of Chemistry, Mersin
University, Mersin, Turkey

Correspondence
Erdal Yabalak, Department of Chemistry,
Mersin University, 33343, Mersin, Turkey.
Email: yabalakerdal@gmail.com

Abstract

This study evaluates the production of hydrochars from the outer shells of the nut group (peanut, hazelnut, walnut, and pistachio) in an eco-friendly subcritical water medium (SWM) and their effects as adsorbents on the removal of crystal violet (CV) from an aqueous solution. The prepared hydrochars were characterized using Brunauer Emmett–Teller (BET) analysis, scanning electron microscope (SEM), Fourier transforms infrared spectroscopy (FTIR), and zeta potential. The adsorption process was optimized based on pH, adsorbent dose, dye concentration, and contact time. The hazelnut hydrochar was found to have the maximum removal efficiency (91%). Optimum conditions were pH of 8, particle size <45 μm, adsorption time of 60 min, and dye concentration of 25 mg/L. The results of all hydrochars were fitted to the second-order kinetics. Langmuir, Freundlich, and Redlich–Peterson isotherms models were used to explain the relationship between adsorbent and adsorbate. For all hydrochars, CV adsorption was found to be feasible and inherently spontaneous. The use of materials with no commercial value like; the outer shells of the nut group, is considered a method for waste reduction using the SWM method.

Practitioner Points

- Hydrochars of nut group were synthesized in the subcritical water medium.
- Adsorption ability of the hydrochars in the adsorption of crystal violet were investigated.
- Adsorption isotherms were used to explain the relationship between adsorbent and adsorbate.
- The hazelnut hydrochar provided the maximum removal efficiency (91%).
- Hazardous water pollutant effectively removed using an eco-friendly method.

KEYWORDS

adsorption, crystal violet, hydrochar production, nut group waste materials

INTRODUCTION

Contamination of the aquatic system by dyes raises concerns about dyestuff materials and their industries (Samsami et al., 2020). Dyes can be defined as any material that has the purpose of coloring (Saxena & Raja, 2014). They can be classified as natural and synthetic based on their origin. Although natural dyes are ecofriendly materials, the world trends toward synthetic types because of the economic aspects (Moussavi & Mahmoudi, 2009). Currently, many industrial activities utilize and release wastewater containing dyes. The textile industry is the dominant industry that releases dyes for about 54% of existing dye effluents. Dyeing, paper, cosmetic, tannery, and plastic industries also release dyes with their wastewater (De Gisi et al., 2016).

The presence of dyes in the water bodies blocks sunlight and inhibits photochemical reactions that cause a decrease in the percentage of dissolved oxygen (Yaseen & Scholz, 2019). It is known that dyes increase chemical oxygen demand (COD) and biological oxygen demand (BOD) in the water. The increase in COD and BOD adversely affect human health and the environment (Myslak et al., 1991). Until now, several treatment methods have been applied to remove dyes from water bodies. Microorganisms containing different types of bacteria (Pearce et al., 2006), algae (Elumalai & Saravanan, 2016), fungi (Krastanov et al., 2013), and enzymes (Darwesh et al., 2019) were used to biodegrade dyes using biological treatment mechanisms. Coagulation-flocculation (Dotto et al., 2019), advanced oxidation processes (dos Santos et al., 2019; Naje et al., 2017; Patel et al., 2020), membrane techniques (Ocakoglu et al., 2021), and combinations from these technologies (Yabalak et al., 2021; Yatmaz et al., 2017) have also been used for dye removal.

The adsorption process has become more favorable due to its cost advantages and simplicity in design and operation (Salinas et al., 2018). Many researchers have used different materials as adsorbents (Yagub et al., 2014). Activated carbon (Agarwal et al., 2016), zeolite (Brião et al., 2018), bio-adsorbent materials from different sources plant (Saleh et al., 2019), fungal materials (Bouras et al., 2019), agricultural wastes (Dai et al., 2018), starch-capped zinc selenide nanoparticles/AC (Sharifpour et al., 2020), *Pinus eldarica* stalks activated carbon (Jafari et al., 2017), activated carbon with multimodal pore size distribution prepared from Amygdalus scoparia (Bagheri et al., 2019), biochar (Biswas et al., 2020; Qiu et al., 2009), and hydrochar (Abaide et al., 2019; Saleh et al., 2020) are the most prominent materials.

Crystal violet (CV) is a cationic dye that is well soluble in water because it contains sulfonic acid (Canizo et al., 2019). CV is known as methyl violet/basic violet-has been used in different applications. CV is used in the gram bacteria classification, textile industries, food sector, cosmetics, and pH indicating (Abd-Elhamid et al., 2019). Notwithstanding that CV dye has lots of applications, several researchers have warned of its toxic effects (Yao et al., 2015). Among these researches, many low-cost adsorbents have been utilized for CV removal, such as *Centaurea solstitialis* and *Verbascum Thapsus* plants (Yalvaç et al., 2021), grapefruit peel (Saeed et al., 2010), semi-interpenetrated networks hydrogels (Li, 2010), rice husk (Chakraborty et al., 2011), water hyacinth (Rajeswari Kulkarni et al., 2017), jackfruit leaf powder (Saha et al., 2012), ginger waste (Kumar & Ahmad, 2011).

Biochar is a stable solid product with high carbon content obtained from different sources by different methods (Lu et al., 2020). Hydrochar, a stable solid product rich in carbon, with superior properties to biochar obtained by conventional methods such as classical torrefaction, pyrolysis, or gasification processes, can be produced from many types of biomass (Chuntanapum & Matsumura, 2009; Kumar & Gupta, 2009). The subcritical water medium (SWM) provides a unique medium for carbonaceous materials conversion to hydrochar with a relatively high yield compared to the methods mentioned above (Saleh et al., 2020). The extraction of valuable materials from many different matrices, oxidation of hazardous compounds, synthesis of organic and inorganic compounds, and solubility of poorly soluble materials can be achieved in SWM, thanks to the changeable physico-chemical properties of subcritical water (Yabalak, 2018a, 2018b). There is a growing interest in hydrochar production and its use in various environmental processes and agricultural applications (Fang et al., 2014). It is known that hydrochars have a significant adsorption capacity to remove dye contaminants from water (Saleh et al., 2020).
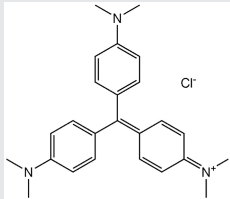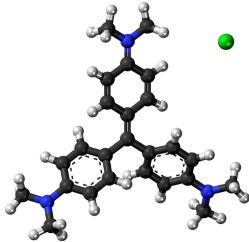
As far as we know, there is no study evaluating the production of hydrochars from the outer shells of the nut group in an eco-friendly SWM medium and their effects as adsorbents on the removal of dye contaminants. Therefore, in this study, the green synthesis of hydrochar based on four different nut materials (peanut, hazelnut, walnut, and pistachio) by SWM was investigated. The ability of the prepared hydrochars to be used as adsorbents for CV removal from the aqueous solutions was investigated.

MATERIAL AND METHOD

Materials

The synthetic dye used (CV) was obtained from Sigma Aldrich. Dye characteristics are shown in Table 1.

TABLE 1 Crystal violet dye characteristics

Chemical formula	$C_{25}H_{30}ClN_3$
Molar mass	407.99 g/mol
2D molecular structure	
3D molecular structure	

Hydrochar materials were collected from Turkey. Hydrochar materials were stored in the laboratory at room temperature until the end of the experiments.

Preparation of hydrochar

Hydrochar production was achieved in the homemade stainless-steel reactor given in previous work (Saleh et al., 2020). Briefly, a homemade stainless steel cylindrical container was used as a reactor, the reactor was heated and stirred using a heater with an integrated magnetic stirrer (Heidolph-MR.3001) and the temperature was controlled by a digital thermometer (Elimko, E-2000). Based on the reactor volume, sufficient amounts of nutshells were added to the reactor each time. Therefore, in each case, 70, 100, 95, and 42 g of dry pistachio, walnut, hazelnut, and peanut shells were used, respectively. The reactor was filled with pure water to a level covering shells. The reactor was closed, pressurized at a constant pressure of 100 bar using N_2 gas, and heated up to 513 K. After a treatment time of 1 h, the reactor was cooled to room temperature, depressurized, and opened. The obtained hydrochars were filtered through ordinary filter paper, dried at 368 K, and weighed. The hydrochar conversion efficiency of the shells was calculated according to the amount of hydrochar obtained using the following Equation 1.

$$Efficiency\ (\%) = \frac{H_o}{S} \times 100 \tag{1}$$

where H_o and S indicate the amount of obtained hydrochar and shell used, respectively. In this study, the efficiencies were 48.6%, 46.1%, 63.2%, and 47.7% for pistachio shell, walnut shell, hazelnut shell and peanut shell, respectively.

Adsorption experiments

The removals of the CV from the aqueous solution onto the prepared hydrochars were assessed via batch experiments. A stock solution with 100-mg/L dye concentration was prepared. All the batch experiments were performed in a 100-mL conical flask containing 50 mL of the dye solution. The agitation speed for all experiments was 155 rpm. The dye concentration in the solution was measured using a UV–Vis spectrophotometer at a wavelength of 590 nm. The removal efficiency and the adsorption capacity were calculated using Equations 2 and 3, respectively (Kasperiski et al., 2018; Mousavi & Seyedi, 2011).

$$qe = \frac{(C0 - Ce)}{m} \times V \tag{2}$$

$$R\,(\%) = \frac{(C0 - Ce)}{C0} \times 100 \tag{3}$$

where C_0 and C_e are initial and equilibrium concentrations of dye (mg/L), respectively, m is the mass of adsorbent (g), V is volume of the solution (L), and q_e is the adsorption capacity (mg/g) (Adelopo et al., 2018).

Kinetic study

For adsorption kinetic studies, 2 g/L of hydrochars were added into 100-mL conical flasks containing 50 mL of CV with different initial concentrations (25, 50, 75 mg/L) and an initial pH value of 8. The mixture was stirred at $25 \pm 2°C$ for 60 min. Then, the adsorbent was separated from the solution by centrifugation at 6000 rpm for 5 min. The concentration of CV in the solution was measured using a UV–visible spectrophotometer at 590 nm. First-order and second-order kinetic models, which were used to describe the adsorption, are shown in Equations 4 and 5, respectively (Pholosi et al., 2019).

$$Log\,(q_e - q_t) = log q_e - \frac{K_1}{2.303}t \tag{4}$$

$$\frac{t}{q_t} = \frac{1}{K_2 q_e^2} + \frac{1}{q_e} t \qquad (5)$$

where q_e and q_t are the capacities of the adsorption at the equilibrium and at time t (mg/g), C_t and C_0 are the initial dye concentration and at any time (mg/L), t is the time (min), K_1 and K_2 are the first-order constant (1/min) and the second-order constant (L/mg. min), respectively.

The intraparticle diffusion model (IDM) proposed by Weber and Morris was also used to explore the diffusion mechanism for the biochars, as shown in Equation 6 (Weber & Morris, 1963).

$$q_t = k_i t^{0.5} + C \qquad (6)$$

where K_i is intraparticle diffusion rate constant (mg g min$^{-1/2}$), C is the constant of the boundary layer thickness.

Adsorption isotherms

The interactions of peanuts, hazelnuts, walnuts, and pistachio-based hydrochars with CV were investigated by isotherms studies. Initial and equilibrium concentrations were used to find the adsorption capacities. The results were fitted to Langmuir (Langmuir, 1918) and Freundlich (Freundlich, 1906) isotherms as two parameters isotherms. Redlich–Peterson isotherm (Redlich & Peterson, 1959) was selected for three-parameters isotherms. The linear forms of Langmuir, Freundlich, and Redlich–Peterson isotherms are shown in Equations 7–9, respectively.

$$\frac{1}{qe} = \frac{1}{Qmax} + \frac{1}{Kl.Qmax.Ce} \qquad (7)$$

$$\log qe = Log\,Kf + \frac{1}{n}\log Ce \qquad (8)$$

$$\ln\left(\frac{KRCe}{qe} - 1\right) = g\,ln(Ce) + ln(a_R) \qquad (9)$$

where K_L is the Langmuir constant (L/mg), $Q_{\max}$ is the maximum adsorption capacity (mg/g), K_f is the Freundlich adsorption capacity parameter (mg/g), (L/mg), 1/n is the intensity parameter, α is the Redlich–Peterson isotherm constant (1/mg), g is the exponent lies between 0 and 1, a_R is R-P isotherm constant (L/g).

Thermodynamic study

For adsorption thermodynamic studies, 2 g/L hydrochar was added to 100-mL conical flasks containing 50 mL of CV at different temperatures (25°C, 30°C, 35°C, 40°C). The mixture was stirred for 60 min until equilibrium was achieved. The adsorbent was then separated from the solution by centrifugation at 6000 rpm for 5 min. The concentration of CV in solution was measured using a UV visible spectrophotometer at 590 nm. The enthalpy changes (ΔH°), entropy (ΔS°), and the Gibbs free energy (ΔG) were found as explained in the previous work (Saleh et al., 2020), as shown in Equations 10–12.

$$\Delta G = -RTLnK_{eq} \qquad (10)$$

$$\Delta G^{\circ} = \Delta H^{\circ} - T\Delta S^{\circ} \qquad (11)$$

$$\ln\frac{C_{Se}}{C_{Ae}} = -\frac{\Delta H}{RT} + \frac{\Delta S}{R} \qquad (12)$$

where K_{eq} is the equilibrium constant.

Desorption study

Desorption studies for the hydrochar with maximum removal efficiency were done as reported in the previous work (Saleh et al., 2019). Briefly, the desorption processes were carried at the end of the adsorption, where the adsorbent separated from the aqueous solution. Four acid types (HCl, H$_2$SO$_4$, HNO$_3$, and H$_3$PO$_4$) and sodium hydroxide (NaOH) were utilized to examine the effect of acid/base type. The desorption was also done at different molarities. The desorption efficiency was calculated using Equation 13;

$$Desorption\,Efficiency(\%) = \frac{Desorbed\,Dye\,Concentration}{Adsorbed\,Dye\,Concentration} \times 100 \qquad (13)$$

Adsorbent characterization

Hydrochar materials were characterized to explore the differences between the samples. Surface charges of the adsorbent at different pHs were measured using zeta potential (Malvern Zeta Sizer Nano ZS). Fourier transform infrared spectroscopy (FTIR) spectra of the adsorbents were recorded via a PerkinElmer (USA) FTIR spectrometer. Surface area, total pore volume, and pore

diameters were measured by Brunauer Emmett–Teller analysis (BET, MicroActive for TriStar II Plus 2.00). The surfaces morphologies for adsorbents were observed by scanning electron microscopy (SEM, Zeiss Supra 55, Germany).

RESULT AND DISCUSSION

Characterization of hydrochar samples

Hydrochars prepared from different nuts sources were characterized using BET analysis (Figure 1). The surface area, total pore volume area, micropore volume, and pore diameter for four different hydrochars are shown in Table 2.

Hazelnut has a maximum surface area of 47.01 m^2/g. Peanut, walnut, and pistachio have surface areas of 6.95, 7.41, and 5.06 m^2/g, respectively. For hazelnut, the total pore volume and the micropore volume are the largest, while the walnut has the largest pore diameter of 20.73 nm.

Changes in the surface morphology of the adsorbents were scanned by SEM images (Figure 2). The peanut-based hydrochar has a heterogenic rough lumpy surface (Figure 2a). After the adsorption process, the surface of the peanut-based hydrochar became smother and lumps disappeared (Figure 2b). The hazelnut based hydrochar has also a relative heterogenic surface with wave-shaped bumps (Figure 2c). Adsorption of CV covered the surface bumps and accumulated the dyes on the surface as shown in Figure 2d. The surface of walnut-based hydrochar formed from the heterogenic accumulated particle with lumps in the top facade (Figure 2e). At the end of the adsorption process, the surface became rougher and more heterogenous indicating the presence of the accumulated dye layers (Figure 2f). Figure 2g shows that the pistachio-based hydrochar has a surface with intense pores, which is filled with CV dye at the end of the adsorption process (Figure 2h).

The FTIR analysis for the hazelnut-based hydrochar before and after the CV adsorption was conducted. Figure 3 shows the FTIR spectra of the raw hydrochar and after the adsorption process. The number of recorded
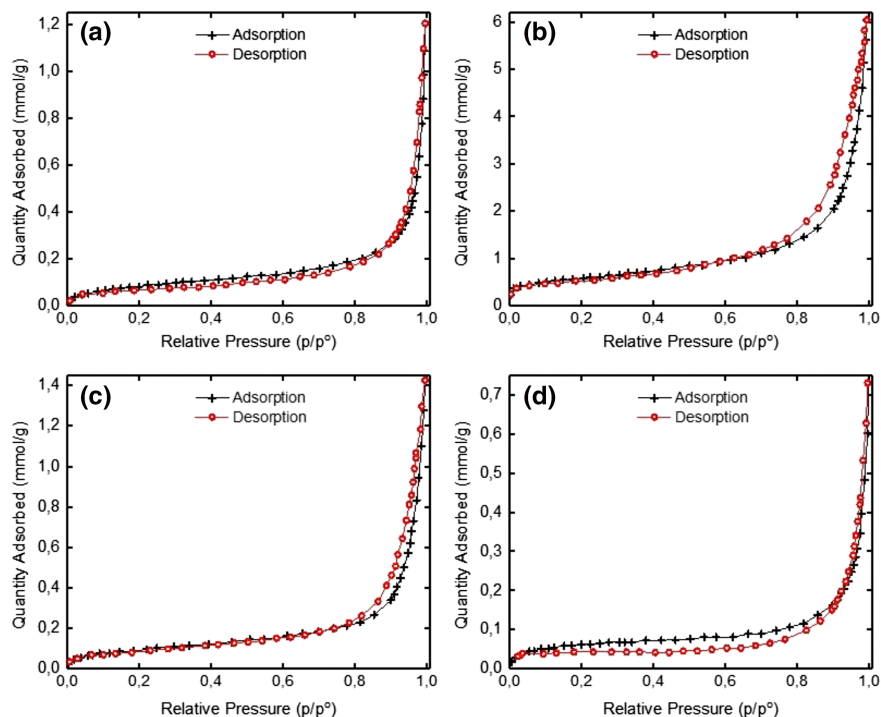

FIGURE 1 N_2 adsorption–desorption curve for (a) peanut, (b) hazelnut, (C) walnut, and (D) pistachio

TABLE 2 The results of BET analysis for the different hydrochar

Properties	Unit	Peanut	Hazelnut	Walnut	Pistachio
Surface area	m^2/g	6.9470	47.0104	7.4109	5.0631
Total pore volume	cm^3/g	0.0271	0.1792	0.0384	0.0169
Micro pore volume	cm^3/g	0.0153	0.1157	0.0235	0.0095
Pore diameter	nm	15.5941	15.2458	20.7322	13.3286
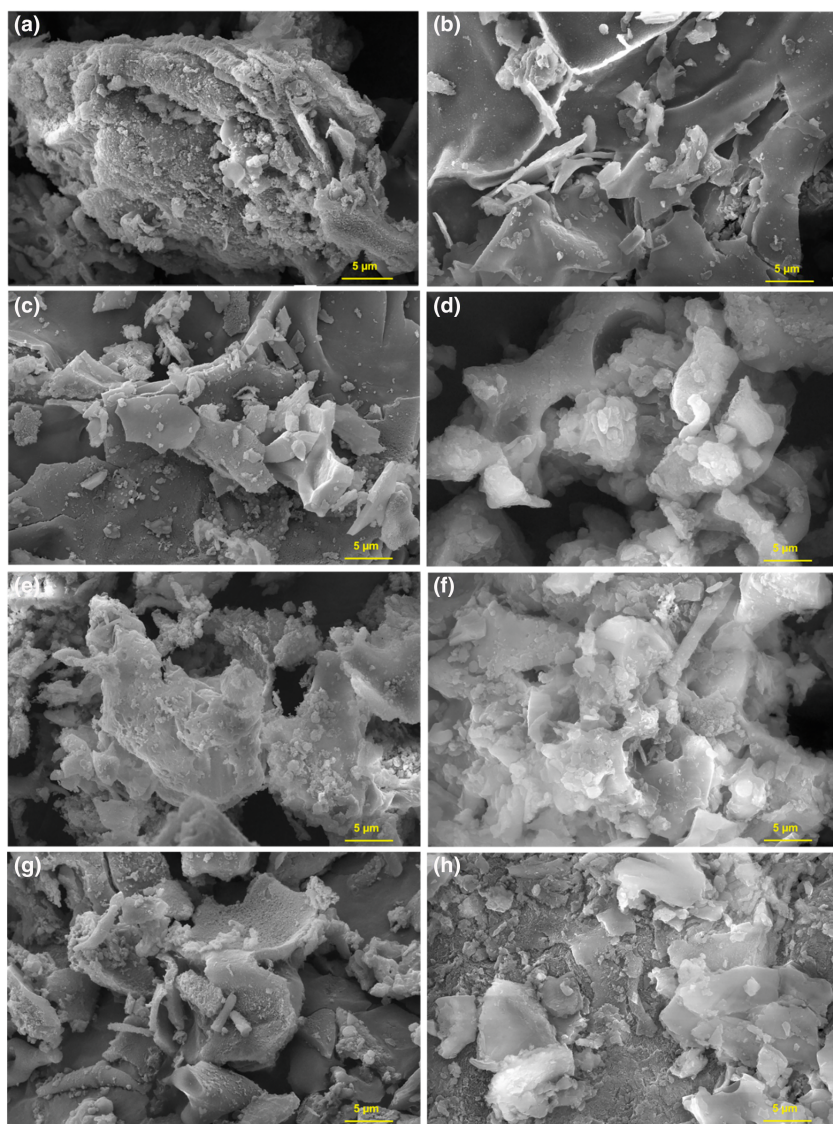
FIGURE 2 Scanning electron microscope (SEM) images of (a) peanut before adsorption, (b) peanut after adsorption, (c) hazelnut before adsorption, (d) hazelnut after adsorption, (e) walnut before adsorption, (f) walnut after adsorption, (g) pistachio before adsorption, and (h) pistachio after adsorption

peaks is higher than five peaks designating that the hydrochar are not simple chemicals. For the raw hydrochars, the broadband near 3300 cm^{-1} indicates the functional group O-H stretching. However, the appearance of sharp intensities in the frequency regions 3666 cm^{-1} means that the hydrochar contains an oxygen-related group. The narrow bands just below 2971 cm^{-1} present the aliphatic compounds with the functional group of C-H stretching. The peaks observed at wavelengths near 2382 cm^{-1} can be related to carbon dioxide compound class and the group O=C=O stretching. The aromatic rings were detected as two sets of absorption bands around 1594 and 1512 cm^{-1}. The functional group for the detected aromatic rings is C-H bending vibration. The peaks recorded between 1408 and 1228 cm^{-1} may be related to O-H bending. The strong peaks near 1065 cm^{-1} may be referred to as C-O stretching. After the adsorption process, many changes were noticed. In general, two new strong peaks were recorded at 1584 and

1028 cm^{-1}. They were related to N-O stretching and C-O stretching, respectively. These peaks were identified after the CV adsorption. The peaks are shreds of evidence for CV adsorption since the CV contains nitrogen and carbon in its structure. For peanut-based hydrochar, the intensities of the adsorption bands just near 3000 cm^{-1} were decreased in half (data not shown). The peak at 2970 cm^{-1} in the walnut hydrochar disappeared after the adsorption (data not shown). In contrast, a new peak was detected near 1690 cm^{-1}, which was related to C=N stretching. For these peaks, pistachio hydrochar had similar results (data not shown). Additionally, a new adsorption band was noticed near 1360 cm^{-1}.

The effect of particle size

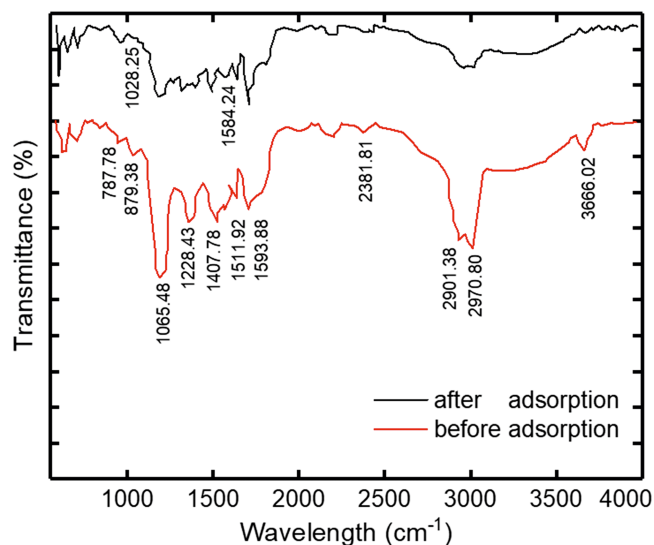The effects of particle sizes on the adsorption efficiencies were determined for the four hydrochar samples. The

FIGURE 3 Fourier transforms infrared spectroscopy (FTIR) analysis for the prepared hazelnut-based hydrochar (a) before the adorption and (b) after the adsorption
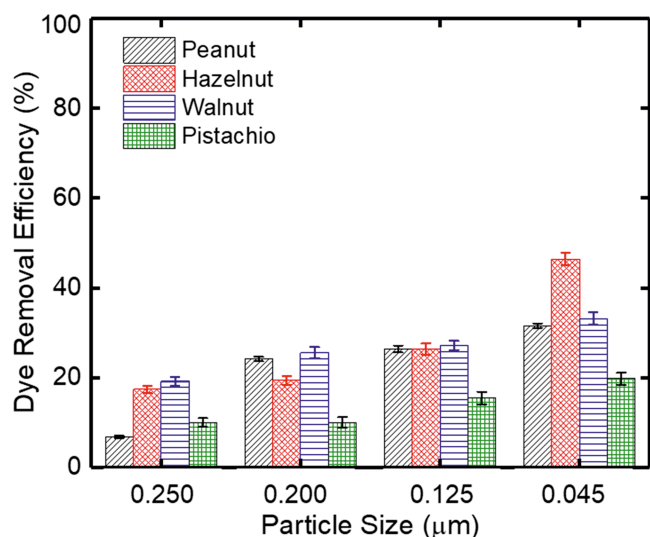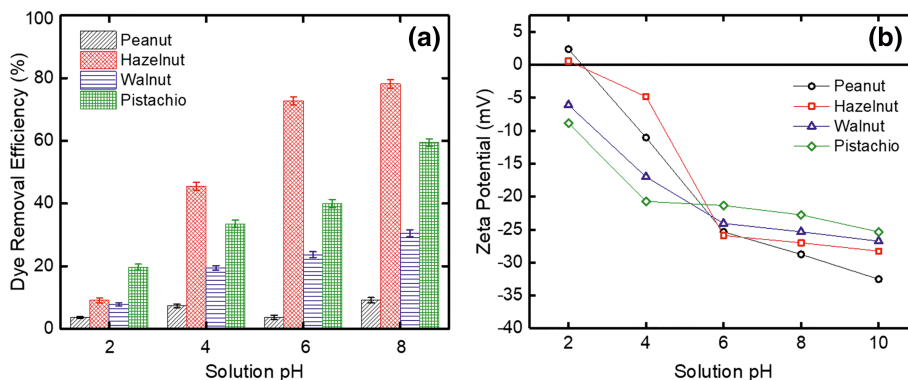

FIGURE 4 Particle size optimization

hydrochars were divided into four main categories according to the sieves they passed. The adsorption process was done in a 100-mL flask containing a 50-mL dye solution with a concentration of 50-mg/L and 1-g/L adsorbent. All samples were agitated at 155 rpm for 1 h at room temperature (25 ± 2°C). The removal efficiencies were calculated and represented in Figure 4. In all samples, the removal efficiencies increased with the reduction in particle size. The decreases in the particle sizes increase the surface area and positively affect the removal efficiency. Similar results were obtained in the previous work (Brião et al., 2018).

The effect of pH

The protonation and deprotonation process during the adsorption process is controlled by the pH values. Thus, it is necessary to optimize the solution pH. Optimization experiments were done using 1 g/L adsorbent added to 50-mg/L CV contained in a 100-mL flask. The flask was shaken at 150 rpm for 1 h at room temperature (25 ± 2°C). The removal efficiencies corresponding to the pH values are shown in Figure 5a. For all hydrochar prepared, the removal efficiencies increased with the increase in the pH values. The same trend was noticed when unburned carbon as a low-cost was utilized as an adsorbent for methylene blue (Wang et al., 2005). The removal efficiencies for peanut and hazelnut incremented from 4% and 9% at pH 2 to 9% and 78% at pH 8, respectively. Walnuts and pistachio hydrochars also showed similar results with maximum removal efficiencies of 31% and 60%, respectively. As shown clearly, hazelnut had the maximum removal efficiency compared to the other hydrochars.

The surface charges of the adsorbents were determined by zeta potential analysis under different pH values (Figure 5b). For all the hydrochars, zeta decreased with the increase of pH. At a lower pH value (pH 2), peanut and hazelnut-based hydrochars had positive values

FIGURE 5 (a) Effect of pH factor on the removal efficiency for the four types of hydrochars and (b) zeta potential values for the adsorbents under different pH values

with a zeta potential of 2.37 and 0.56 mV, respectively. The surface charges for walnut and pistachio-based hydrochars were negative at all pH range. The zeta potential for the four hydrochars ranged from −22.75 to −28.75 mV at pH 8. Negative surface charges on the adsorbent promote the adsorption of a positive dye, CV. At higher pH values, the oxygen deprotonated from the CV, and the surface charges of the hydrochars became more negative. In this way, the adsorption capacity increased (Isik, Saleh, Bilici, et al., 2021).

The effect of contact time

The effect of contact time on the adsorption of CV using the prepared hydrochars was determined. Solutions with a concentration of 50 mg/L were prepared, and the dye uptakes were calculated over time. Figure 6 shows the removal efficiency and the adsorption capacity for the four hydrochars versus time. As observed in the previous works (Isik, Saleh, & Dizge, 2021; Saleh et al., 2020), a sharp increase in the removal efficiencies and the adsorption capacities were observed during the first 5 min when the active surface sites were empty and available. With time increasing, the active site numbers decreased until the removal efficiencies and the adsorption capacities reached the steady-state after 45 min. Hazelnut-based hydrochar had the maximum removal efficiency (92%), and the adsorption capacity was 23 mg/g. Pistachio-based hydrochar followed the hazelnut with a removal efficiency and an adsorption capacity of 73% and 19 mg/g, respectively. The removal efficiency and the adsorption capacity for the walnut-based hydrochar were 66% and 17 mg/g, respectively. The peanut-based hydrochar showed the minimum efficiency (60%) and the adsorption capacity (15 mg/g). For all the prepared hydrochars, the adsorption capacities are higher than obtained from the granular activated carbon prepared from fruit stones and nutshells by Aygün et al. (2003).

Kinetic studies

The kinetic studies for the adsorption of CV onto the prepared hydrochars were done at different concentrations. The obtained results were fitted to Lagergren's pseudo-first-order and pseudo-second-order models. The correlation factors and the chi-square error test (X^2) were used to justify the best model. Table 3 shows the two kinetic models and their parameters, as well as the statistical results.

For all the prepared hydrochars, the pseudo-second-order model showed higher correlation coefficients and smaller X^2 error values. Accordingly, the adsorptions of CV onto the different hydrochars' samples were described by the pseudo-second-order model. The pseudo-second-order model can describe the adsorption process over the whole contact times, which is not present in Lagergren's pseudo-first-order. In the pseudo-second-order model, the increase in the adsorption of CV is proportional to the presence of the active sites on the hydrochars surface. Guo and Wang (2019) explored the mechanism of the adsorption due to the pseudo-second-order model. Accordingly, the adsorption may occur at low concentrations, at the final steps of the adsorption, and when the surface of the adsorbent is rich with the active sites (Guo & Wang, 2019).

The diffusion effects on the adsorption of CV onto the prepared hydrochars by the IDM. Figure 7 shows the IDM for CV adsorption onto the prepared hydrochars. For all hydrochars, the IDM plots had multiple linear sections, which reflects the presence of different mechanisms. The film diffusion was the first mechanism when the CV moved from the boundary layer to the hydrochars surfaces. The movement from the surfaces toward the pores and the attachment with available sites were the other mechanisms. The multilinearity reflects the role of intraparticle resistance in CV adsorption. Also, the IDM lines were not passed through the origin point since that film diffusion is the dominant mechanism in CV adsorption.
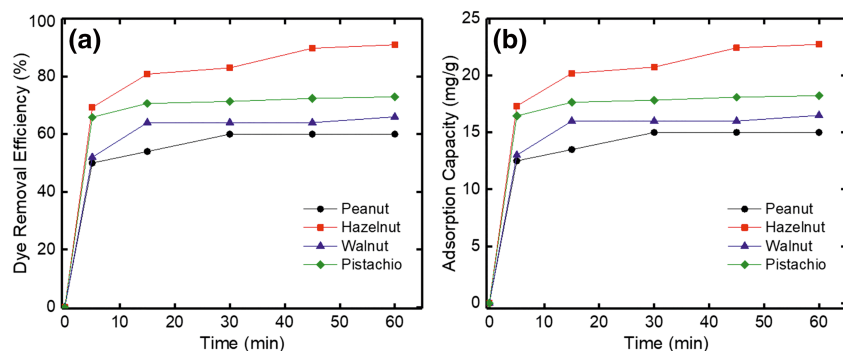
FIGURE 6 (a) The removal efficiency changes with the concentration over time and (b) the adsorption capacities changes related to the initial concentration

TABLE 3 1st order and 2nd order kinetic model fit results for peanuts, hazelnuts, walnuts, and pistachio hydrochars

|	Concentration (mg/L)	1st order					2nd order				
		K_1	q_e measured (mg/g)	q_e fitted (mg/g)	R^2	X^2	k_2	q_e measured (mg/g)	q_e fitted (mg/g)	R^2	X^2
Peanut	10	0.194	3.06	2.406	0.961	0.786	0.055	3.060	3.238	0.997	0.389
	25	0.152	7.90	7.202	0.701	5.151	0.098	7.901	7.857	0.996	0.137
	50	0.181	4.46	15.100	0.783	4.757	0.055	15.100	15.174	0.999	8.65E−03
Hazelnut	10	0.239	4.65	1.946	0.796	7.688	4.69E−01	4.651	4.639	0.999	4.82E−02
	25	0.258	7.03	11.975	0.952	1.764	9.39E−02	11.975	12.088	0.999	0.014
	50	0.271	22.74	20.935	0.887	4.880	3.01E−02	22.745	22.984	0.997	1.23E−02
Walnut	10	0.239	4.41	8.607	0.770	8.959	1.54E−01	4.411	4.449	0.998	1.84E−01
	25	0.251	11.11	4.905	0.942	2.020	8.19E−02	11.299	11.110	0.999	0.0025
	50	0.219	16.51	7.667	0.815	5.688	4.91E−02	16.51	16.701	0.999	4.20E−03
Pistachio	10	0.265	4.726	1.254	0.901	4.023	5.57E−01	4.726	4.751	0.999	1.21E−03
	25	0.223	11.31	4.755	0.918	2.323	8.71E−02	11.555	11.457	0.999	0.00139
	50	0.298	18.236	9.038	0.866	7.141	7.81E−02	18.236	18.401	0.999	3.13E−04
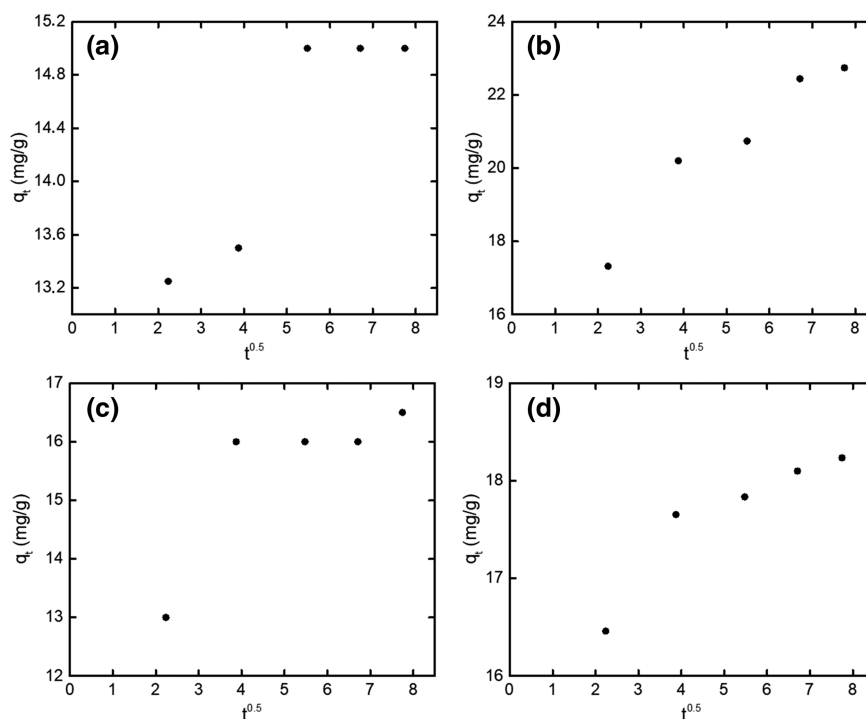
FIGURE 7 The intraparticle diffusion model (IDM) plots for (a) peanut, (b) hazelnut, (c) walnut, and (d) pistachio

Isotherms

The adsorption isotherms for the CV dyes onto the prepared hydrochar were studied. The adsorption processes were done at room temperature ($25 \pm 2°C$) for 1 h at an agitation speed of 155 rpm. At the end of the adsorption process, the obtained samples were fitted to the Langmuir, Freundlich, and Redlich–Peterson isotherms. The linear forms of the three isotherms were

fitted and shown in Table 4. According to Table 4, the results were found to be in a good fit with both Langmuir and Redlich–Peterson isotherms. In contrast, Freundlich isotherm, which assumes the heterogeneity of the adsorption, had lower correlation coefficients. Langmuir isotherm showed a correlation coefficient of 0.999 for the pistachio-based hydrochar. Langmuir explains the formation of a homogenous monolayer at the saturation conditions. Redlich–Peterson had the

Isotherm	Parameter	Peanut	Hazelnut	Walnut	Pistachio
Langmuir	Q_{max}	32.700	38.649	19.523	20.839
	K_L	0.019	0.322	0.359	0.507
	R^2	0.990	0.872	0.898	0.999
Freundlich	n	1.062	1.343	2.209	2.395
	K_f	1.130	8.011	5.071	6.636
	R^2	0.978	0.834	0.828	0.955
Redlich–Peterson	K_R	20.000	25.000	15.000	22.000
	g	0.267	0.191	0.617	0.716
	a_R	12.398	2.951	2.244	2.233
	R^2	0.996	0.999	0.906	0.991

TABLE 4 Langmuir, Freundlich, and Redlich–Peterson isotherms parameter of the adsorption of CV onto the different hydrochars

Hydrochar	T (°C)	T (K)	ΔH (kJ/mol)	ΔS (J/mol K)	ΔG (kJ/mol)
Peanut	25	298	8.618	34.057	−1.531
	30	303			−1.701
	35	308			−1.871
	40	313			−2.042
Hazelnut	25	298	11.689	42.318	−0.923
	30	303			−1.135
	35	308			−1.346
	40	313			−1.558
Walnut	25	298	8.510	29.432	−0.261
	30	303			−0.408
	35	308			−0.555
	40	313			−0.702
Pistachio	25	298	9.136	32.696	−0.607
	30	303			−0.771
	35	308			−0.934
	40	313			−1.098

TABLE 5 Gibbs free energy, enthalpy, and entropy results of the adsorption of CV onto peanuts, hazelnuts, walnuts, and pistachio hydrochars

maximum correlation coefficients for the peanut (0.996), hazelnut (0.999), and walnut (0.906). In these nuts, the adsorption mechanism is a mixture between the Langmuir and Freundlich isotherms. Redlich–Peterson stated that no ideal monolayer did not form at the adsorbent surface.

Thermodynamic

The adsorptions of CV onto the peanut, hazelnut, walnut, and pistachio-based hydrochar were investigated based on the thermodynamic concept. Gibb's free energy, enthalpy, and entropy for the adsorptions processes were found by conducting the adsorption under different temperatures (298, 303, 308, and 313 K). Table 5 presents the thermodynamic parameters for the four hydrochars.

For all the prepared hydrochars, the adsorption of CV was found to be feasible and naturally spontaneous because of the negative sign of Gibb's free energy. With the increases in the temperatures, the negative sign of the Gibbs free energy also increased. Peanuts-based hydrochar had the highest Gibbs free energy followed by hazelnuts hydrochar, while the peanuts-based hydrochar had the minimum value for the Gibbs free energy. For the four hydrochars, the adsorption of CV from the aqueous solutions can be considered to be physisorption, because the Gibbs free energy is lower than 20 kJ/mol

(Guo & Wang, 2019). The enthalpies for the adsorption process of CV have positive values, which indicates that the adsorption is endothermic. The entropy values for the hydrochars are positives, which hint that the interface between the adsorbent and the adsorbate has become more random. Similar results were obtained previously (Biswas et al., 2020; Dawood et al., 2017; Singh & Kaur, 2013).
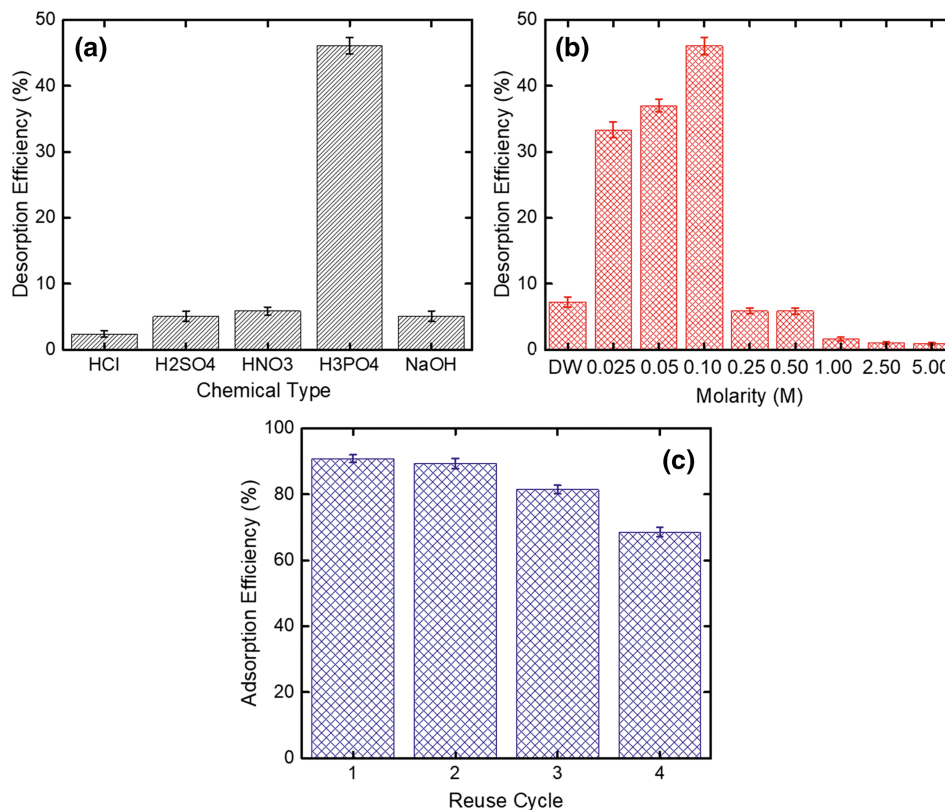
FIGURE 8 Adsorption–desorption studies of crystal violet (CV) dye using hazelnut-based hydrochar (a) the effect of acid and base type on CV dye desorption, (b) the effect of phosphoric acid molarity on CV dye desorption, and (c) adsorption–desorption cycle

TABLE 6 Comparison with other studies

Raw material	Adsorbate	Capacity (mg/g)	Isotherm	Kinetic	Thermodynamic	Ref.
Hazelnut-based hydrochar	Crystal violet	32.7	Redlich–Peterson	Pseudo-second order	Endothermic	This study
Palm kernel fiber	Crystal violet	78.9	Freundlich	Pseudo-second order	Endothermic	(El-Sayed, 2011)
Palm petiole	Crystal violet	209.0	Langmuir	Empiric Avrami	Endothermic	(Fang et al., 2014)
Nano-hazelnut shell	Crystal violet	294.12	Langmuir	—	Exothermic	(Al-Ajji & Al-Ghouti, 2021)
Sterculia alata fruit Shell biochar	Patent blue V	11.4	Freundlich	Pseudo-first-order	—	(Giri et al., 2017)
Cashew nut shell	Congo red	5.2	Redlich–Peterson	Pseudo-second order	Exothermic	(Senthil Kumar et al., 2010)
Oil palm wastes-derived activated carbons	Methylene blue	24.0	Langmuir	Pseudo-second order	—	(Baloo et al., 2021)

Desorption study

By comparison among the four types of prepared hydrochars, hazelnut-based hydrochar showed the best removal efficiency in the adsorption process. So, the desorption study was conducted for the hazelnut-based hydrochar only at the optimum conditions (adsorbent amount of 2 g/L, CV dye concentration of 50 mg/L, pH of 8, and a contact time of 60 min). The maximum desorption was obtained when the phosphoric acid was used with a molarity of 0.1 M (Figure 8a). The maximum recovery was 46.1% (Figure 8b). The adsorption–desorption experiments were revolved four times to examine the reusability of the adsorbent. Figure 8c shows the removal efficiency for each cycle. The removal efficiency of CV by the hazelnut-based hydrochar decreased from 90.86% in the first cycle to 68.62% in the fourth cycle. The hydrochar was successfully utilized for three cycles.

Comparison with other adsorbents

The removal efficiency and the adsorption capacity for the prepared hydrochars in this study were compared with previous studies, as shown in Table 6.

CONCLUSION

In this study, the production of peanut, hazelnut, walnut, and pistachio-based hydrochars by the eco-friendly SWM method was investigated. The prepared hydrochars were utilized in CV dye removal from an aqueous solution using the adsorption method. The optimum conditions were pH of 8, particle size <45 μm, contact time of 60 min, and CV concentration of 25 mg/L. The hazelnut-based hydrochar was found to have the maximum removal efficiency (91%). For all the prepared hydrochars, the adsorption of CV was found to be feasible and naturally spontaneous. At the end of this study, we can conclude that the subcritical water medium (SWM) provides a unique medium for carbonaceous materials conversion into hydrochar with a relatively high yield. Also, the use of materials with no commercial value like; the outer shells of the nut group, is viewed as a waste reduction method.

CONFLICT OF INTEREST
No potential conflict of interest was reported by the authors.

AUTHOR CONTRIBUTIONS
Mohammed Saleh: Conceptualization; data curation; formal analysis; investigation; methodology; validation; visualization. **Zelal Isik:** Formal analysis; investigation; methodology. **Erdal Yabalak:** Conceptualization; data curation; formal analysis; investigation; methodology; resources; supervision; validation; visualization. **Mutlu Yalvac:** Formal analysis; resources. **Nadir Dizge:** Conceptualization; data curation; formal analysis; investigation; methodology; resources; supervision; validation; visualization.

ORCID
Erdal Yabalak https://orcid.org/0000-0002-4009-4174
Nadir Dizge https://orcid.org/0000-0002-7805-9315

REFERENCES

Abaide, E. R., Dotto, G. L., Tres, M. V., Zabot, G. L., & Mazutti, M. A. (2019). Adsorption of 2–nitrophenol using rice straw and rice husks hydrolyzed by subcritical water. *Bioresource Technology*, *284*, 25–35. https://doi.org/10.1016/j.biortech.2019.03.110

Abd-Elhamid, A. I., Fawal, G. F., & Akl, M. A. (2019). Methylene blue and crystal violet dyes removal (as a binary system) from aqueous solution using local soil clay: Kinetics study and equilibrium isotherms. *Egyptian Journal of Chemistry*, *62*, 541–554.

Adelopo, A., Haris, P., Alo, B., Huddersman, K., & Jenkins, R. (2018). Conversion of solid waste to activated carbon to improve landfill sustainability. *Waste Manag. Res. J. a Sustain. Circ. Econ.*, *36*, 708–718. https://doi.org/10.1177/0734242X18788940

Agarwal, S., Tyagi, I., Gupta, V. K., Bagheri, A. R., Ghaedi, M., Asfaram, A., Hajati, S., & Bazrafshan, A. A. (2016). Rapid adsorption of ternary dye pollutants onto copper (I) oxide nanoparticle loaded on activated carbon: Experimental optimization via response surface methodology. *Journal of Environmental Chemical Engineering*, *4*, 1769–1779. https://doi.org/10.1016/j.jece.2016.03.002

Al-Ajji, M. A., & Al-Ghouti, M. A. (2021). Novel insights into the nanoadsorption mechanisms of crystal violet using nanohazelnut shell from aqueous solution. *Journal of Water Process Engineering*, *44*, 102354. https://doi.org/10.1016/j.jwpe.2021.102354

Aygün, A., Yenisoy-Karakaş, S., & Duman, I. (2003). Production of granular activated carbon from fruit stones and nutshells and evaluation of their physical, chemical and adsorption properties. *Microporous and Mesoporous Materials*, *66*(2–3), 189–195. https://doi.org/10.1016/j.micromeso.2003.08.028

Bagheri, R., Ghaedi, M., Asfaram, A., Dil, E. A., & Javadian, H. (2019). RSM-CCD design of malachite green adsorption onto activated carbon with multimodal pore size distribution prepared from Amygdalus scoparia: Kinetic and isotherm studies. *Polyhedron*, *171*, 464–472. https://doi.org/10.1016/j.poly.2019.07.037

Baloo, L., Isa, M. H., Bin Sapari, N., Jagaba, A. H., Wei, L.J., Yavari, S., Razali, R., & Vasu, R. (2021). Adsorptive removal of methylene blue and acid orange 10 dyes from aqueous solutions using oil palm wastes-derived activated carbons. *Alexandria Engineering Journal*, *60*(6), 5611–5629. https://doi.org/10.1016/j.aej.2021.04.044

Biswas, S., Mohapatra, S. S., Kumari, U., Meikap, B. C., & Sen, T. K. (2020). Batch and continuous closed circuit semi-fluidized bed operation: Removal of MB dye using sugarcane bagasse biochar and alginate composite adsorbents. *Journal of Environmental Chemical Engineering*, *8*, 103637. https://doi.org/10.1016/j.jece.2019.103637

Bouras, H. D., Isik, Z., Bezirhan Arikan, E., Bouras, N., Chergui, A., Yatmaz, H. C., & Dizge, N. (2019). Photocatalytic oxidation of azo dye solutions by impregnation of ZnO on fungi. *Biochemical Engineering Journal*, *146*, 150–159. https://doi.org/10.1016/j.bej.2019.03.014

Brião, G. V., Jahn, S. L., Foletto, E. L., & Dotto, G. L. (2018). Highly efficient and reusable mesoporous zeolite synthetized from a biopolymer for cationic dyes adsorption. *Colloids Surfaces a Physicochem. Eng. Asp.*, *556*, 43–50. https://doi.org/10.1016/j.colsurfa.2018.08.019

Canizo, B. V., Agostini, E., Oller, A. L., Dotto, G. L., Vega, I. A., & Escudero, L. B. (2019). Removal of crystal violet from natural water and effluents through biosorption on bacterial biomass isolated from rhizospheric soil. *Water, Air, & Soil Pollution*, *230*(8), 1–14. https://doi.org/10.1007/s11270-019-4235-5

Chakraborty, S., Chowdhury, S., & Saha, P. D. (2011). Adsorption of crystal violet from aqueous solution onto NaOH-modified rice husk. *Carbohydrate Polymers*, *86*(4), 1533–1541. https://doi.org/10.1016/j.carbpol.2011.06.058

Chuntanapum, A., & Matsumura, Y. (2009). Formation of tarry material from 5-HMF in subcritical and supercritical water. *Industrial and Engineering Chemistry Research*, *48*, 9837–9846. https://doi.org/10.1021/ie900423g

Dai, Y., Sun, Q., Wang, W., Lu, L., Liu, M., Li, J., Yang, S., Sun, Y., Zhang, K., Xu, J., Zheng, W., Hu, Z., Yang, Y., Gao, Y., Chen, Y., Zhang, X., Gao, F., & Zhang, Y. (2018). Utilizations of agricultural waste as adsorbent for the removal of contaminants: A review. *Chemosphere*, *211*, 235–253. https://doi.org/10.1016/j.chemosphere.2018.06.179

Darwesh, O. M., Matter, I. A., & Eida, M. F. (2019). Development of peroxidase enzyme immobilized magnetic nanoparticles for bioremediation of textile wastewater dye. *Journal of Environmental Chemical Engineering*, *7*, 102805. https://doi.org/10.1016/j.jece.2018.11.049

Dawood, S., Sen, T. K., & Phan, C. (2017). Synthesis and characterization of slow pyrolysis pine cone bio-char in the removal of organic and inorganic pollutants from aqueous solution by adsorption: Kinetic, equilibrium, mechanism and thermodynamic. *Bioresource Technology*, *246*, 76–81. https://doi.org/10.1016/j.biortech.2017.07.019

De Gisi, S., Lofrano, G., Grassi, M., & Notarnicola, M. (2016). Characteristics and adsorption capacities of low-cost sorbents for wastewater treatment: A review. *Sustainable Materials and Technologies*, *9*, 10–40. https://doi.org/10.1016/j.susmat.2016.06.002

dos Santos, A. J., Garcia-Segura, S., Dosta, S., Cano, I. G., Martínez-Huitle, C. A., & Brillas, E. (2019). A ceramic electrode of ZrO2-Y2O3 for the generation of oxidant species in anodic oxidation. Assessment of the treatment of Acid Blue 29 dye in sulfate and chloride media. *Separation Purification Technology*, *228*, 115747. https://doi.org/10.1016/j.seppur.2019.115747

Dotto, J., Fagundes-Klen, M. R., Veit, M. T., Palácio, S. M., & Bergamasco, R. (2019). Performance of different coagulants in the coagulation/flocculation process of textile wastewater. *Journal of Cleaner Production*, *208*, 656–665. https://doi.org/10.1016/j.jclepro.2018.10.112

El-Sayed, G. O. (2011). Removal of methylene blue and crystal violet from aqueous solutions by palm kernel fiber. *Desalination*, *272*(1–3), 225–232. https://doi.org/10.1016/j.desal.2011.01.025

Elumalai, S., & Saravanan, G. K. (2016). The role of microalgae in textile dye industrial waste water recycle (phycoremediation). *International Journal Pharma & Bio Sciences*, *7*, 662–673.

Fang, G., Gao, J., Liu, C., Dionysiou, D. D., Wang, Y., & Zhou, D. (2014). Key role of persistent free radicals in hydrogen peroxide activation by biochar: Implications to organic contaminant degradation. *Environmental Science & Technology*, *48*, 1902–1910. https://doi.org/10.1021/es4048126

Freundlich, H. M. F. (1906). Over the adsorption in solution. *The Journal of Physical Chemistry*, *57*, 385–471.

Giri, B. S., Goswami, M., Kumar, P., Yadav, R., Sharma, N., Sonwani, R. K., Yadav, S., Singh, R. P., Rene, E. R., Chaturvedi, P., & Singh, R. S. (2017). Adsorption of patent blue v from textile industry wastewater using *sterculia alata* fruit shell biochar: Evaluation of efficiency and mechanisms. *Water*, *2020*, 12. https://doi.org/10.3390/w12072017

Guo, X., & Wang, J. (2019). A general kinetic model for adsorption: Theoretical analysis and modeling. *Journal of Molecular Liquids*, *288*, 111100. https://doi.org/10.1016/j.molliq.2019.111100

Isik, Z., Saleh, M., Bilici, Z., & Dizge, N. (2021). Remazol brilliant blue R (RBBR) dye and phosphate adsorption by calcium alginate beads modified with polyethyleneimine. *Water Environment Research*, *93*, 1–15. https://doi.org/10.1002/wer.1635

Isik, Z., Saleh, Z., & Dizge, N. (2021). Adsorption studies of ammonia and phosphate ions onto calcium alginate beads. *Surfaces and Interfaces*, *26*, 101330. https://doi.org/10.1016/j.surfin.2021.101330

Jafari, M., Rahimi, M. R., Ghaedi, M., Javadian, H., & Asfaram, A. (2017). Fixed-bed column performances of azure-II and auramine-O adsorption by Pinus eldarica stalks activated carbon and its composite with zno nanoparticles: Optimization by response surface methodology based on central composite design. *Journal of Colloid and Interface Science*, *507*, 172–189. https://doi.org/10.1016/j.jcis.2017.07.056

Kasperiski, F. M., Lima, E. C., Umpierres, C. S., dos Reis, G. S., Thue, P. S., Lima, D. R., Dias, S. L. P., Saucier, C., & da Costa, J. B. (2018). Production of porous activated carbons from Caesalpinia ferrea seed pod wastes: Highly efficient removal of captopril from aqueous solutions. *Journal of Cleaner Production*, *197*, 919–929. https://doi.org/10.1016/j.jclepro.2018.06.146

Krastanov, A., Koleva, R., Alexieva, Z., & Stoilova, I. (2013). Decolorization of industrial dyes by immobilized mycelia of Trametes versicolor. *Biotechnology and Biotechnological Equipment*, *27*, 4263–4268. https://doi.org/10.5504/BBEQ.2013.0096

Kumar, R., & Ahmad, R. (2011). Biosorption of hazardous crystal violet dye from aqueous solution onto treated ginger waste (TGW). *Desalination*, *265*(1), 112–118. https://doi.org/10.1016/j.desal.2010.07.040

Kumar, S., & Gupta, R. B. (2009). Biocrude production from switchgrass using subcritical water. *Energy & Fuels*, *23*, 5151–5159. https://doi.org/10.1021/ef900379p

Langmuir, I. (1918). The adsorption of gases on plane surfaces of glass, mica and platinum. *J. Am. Chemical Society*, *40*, 1361–1403. https://doi.org/10.1021/ja02242a004

Li, S. (2010). Removal of crystal violet from aqueous solution by sorption into semi-interpenetrated networks hydrogels constituted of poly (acrylic acid-acrylamide-methacrylate) and amylose. *Bioresource Technology*, *101*(7), 2197–2202. https://doi.org/10.1016/j.biortech.2009.11.044

Lu, L., Yu, W., Wang, Y., Zhang, K., Zhu, X., Zhang, Y., Wu, Y., Ullah, H., Xiao, X., & Chen, B. (2020). Application of biochar-based materials in environmental remediation: From multi-level structures to specific devices. *Biochar*, *2*, 1–31. https://doi.org/10.1007/s42773-020-00041-7

Mousavi, H. Z., & Seyedi, S. R. (2011). Nettle ash as a low cost adsorbent for the removal of nickel and cadmium from wastewater. *International Journal of Environmental Science and Technology*, *8*, 195–202. https://doi.org/10.1007/BF03326209

Moussavi, G., & Mahmoudi, M. (2009). Removal of azo and anthraquinone reactive dyes from industrial wastewaters using MgO nanoparticles. *Journal of Hazardous Materials*, *168*, 806–812. https://doi.org/10.1016/j.jhazmat.2009.02.097

Myslak, Z. W., Bolt, H. M., & Brockmann, W. (1991). Tumors of the urinary bladder in painters: A case-control study. *American Journal of Industrial Medicine*, *19*, 705–713. https://doi.org/10.1002/ajim.4700190604

Naje, A. S., Chelliapan, S., Zakaria, Z., Ajeel, M. A., & Alaba, P. A. (2017). A review of electrocoagulation technology for the treatment of textile wastewater. *Reviews in Chemical Engineering*, *33*, 263–292. https://doi.org/10.1515/revce-2016-0019

Ocakoglu, K., Dizge, N., Colak, S. G., Ozay, Y., Bilici, Z., Yalcin, M. S., Ozdemir, S., & Yatmaz, H. C. (2021). Poly-ethersulfone membranes modified with CZTS nanoparticles for protein and dye separation: Improvement of antifouling and self-cleaning performance. *Colloids Surfaces a Physicochemical and Engineering Aspects*, *5*, 126230. https://doi.org/10.1016/j.colsurfa.2021.126230

Patel, S. K., Patel, S. G., & Patel, G. V. (2020). Degradation of reactive dye in aqueous solution by Fenton, photo-Fenton process and combination process with activated charcoal and TiO2. *Proceedings of the National Academy of Sciences, India Section A: Physical Sciences*, *90*, 579–591. https://doi.org/10.1007/s40010-019-00618-3

Pearce, C. I., Christie, R., Boothman, C., von Canstein, H., Guthrie, J. T., & Lloyd, J. R. (2006). Reactive azo dye reduction by Shewanella strain J18 143. *Biotechnology and Bioengineering*, *95*, 692–703. https://doi.org/10.1002/bit.21021

Pholosi, A., Naidoo, E. B., & Ofomaja, A. E. (2019). Enhanced arsenic (III) adsorption from aqueous solution by magnetic pine cone biomass. *Materials Chemistry and Physics*, *222*, 20–30. https://doi.org/10.1016/j.matchemphys.2018.09.067

Qiu, Y., Zheng, Z., Zhou, Z., & Sheng, G. D. (2009). Effectiveness and mechanisms of dye adsorption on a straw-based biochar. *Bioresource Technology*, *100*, 5348–5351. https://doi.org/10.1016/j.biortech.2009.05.054

Rajeswari Kulkarni, M., Revanth, T., Acharya, A., & Bhat, P. (2017). Removal of crystal violet dye from aqueous solution using water hyacinth: Equilibrium, kinetics and thermodynamics study. *Resource-Efficient Technologies*, *3*(1), 71–77. https://doi.org/10.1016/j.reffit.2017.01.009

Redlich, O., & Peterson, D. L. (1959). A useful adsorption isotherm. *The Journal of Physical Chemistry*, *63*, 1024–1024. https://doi.org/10.1021/j150576a611

Saeed, A., Sharif, M., & Iqbal, M. (2010). Application potential of grapefruit peel as dye sorbent: Kinetics, equilibrium and mechanism of crystal violet adsorption. *Journal of Hazardous Materials*, *179*(1), 564–572. https://doi.org/10.1016/j.jhazmat.2010.03.041

Saha, P. D., Chakraborty, S., & Chowdhury, S. (2012). Batch and continuous (fixed-bed column) biosorption of crystal violet by Artocarpus heterophyllus (jackfruit) leaf powder. *Colloids and Surfaces. B, Biointerfaces*, *92*, 262–270. https://doi.org/10.1016/j.colsurfb.2011.11.057

Saleh, M., Yalvaç, M., & Arslan, H. (2019). Optimization of remazol brilliant blue R adsorption onto *Xanthium Italicum* using the response surface method. *Karbala International Journal of Modern Science*, *5*, 53–63. https://doi.org/10.33640/2405-609X.1017

Saleh, M., Bilici, Z., Ozay, Y., Yabalak, E., Yalvac, M., & Dizge, N. (2020). Green synthesis of Quercus coccifera hydrochar in sub-critical water medium and evaluation of its adsorption performance for BR18 dye. *Water Science and Technology*, *83*, 701–714. https://doi.org/10.2166/wst.2020.607

Salinas, T., Durruty, I., Arciniegas, L., Pasquevich, G., Lanfranconi, M., Orsi, I., Alvarez, V., & Bonanni, S. (2018). Design and testing of a pilot scale magnetic separator for the treatment of textile dyeing wastewater. *Journal of Environmental Management*, *218*, 562–568. https://doi.org/10.1016/j.jenvman.2018.04.096

Samsami, S., Mohamadi, M., Sarrafzadeh, M.-H., Rene, E. R., & Firoozbahr, M. (2020). Recent advances in the treatment of dye-containing wastewater from textile industries: Overview and perspectives. *Process Safety and Environment Protection*, *143*, 138–163. https://doi.org/10.1016/j.psep.2020.05.034

Saxena, S., & Raja, A. S. M. (2014). *Natural dyes: Sources* (pp. 37–80). Chemistry. https://doi.org/10.1007/978-981-287-065-0_2

Senthil Kumar, P., Ramalingam, S., Senthamarai, C., Niranjanaa, M., Vijayalakshmi, P., & Sivanesan, S. (2010). Adsorption of dye from aqueous solution by cashew nut shell: Studies on equilibrium isotherm, kinetics and thermodynamics of interactions. *Desalination*, *261*(1–2), 52–60. https://doi.org/10.1016/j.desal.2010.05.032

Sharifpour, E., Ghaedi, M., Asfaram, A., Farsadrooh, M., Dil, E. A., & Javadian, H. (2020). Modeling and optimization of ultrasound-assisted high performance adsorption of basic Fuchsin by starch-capped zinc selenide nanoparticles/AC as a novel composite using response surface methodology. *International Journal of Biological Macromolecules*, *152*, 913–921. https://doi.org/10.1016/j.ijbiomac.2020.02.236

Singh, J., & Kaur, G. (2013). Freundlich, Langmuir adsorption isotherms and kinetics for the removal of malachite green from aqueous solutions using agricultural waste rice straw. *International Journal of Environmental Sciences*, *4*, 250–258. https://doi.org/10.6088/ijes.2013040300004

Wang, S., Li, L., Wu, H., & Zhu, Z. H. (2005). Unburned carbon as a low-cost adsorbent for treatment of methylene blue-containing wastewater. *Journal of Colloid and Interface Science*, *292*(2), 336–343. https://doi.org/10.1016/j.jcis.2005.06.014

Weber, W. J., & Morris, J. C. (1963). Kinetics of adsorption on carbon from solution. *J. Sanit Eng. ASCE*, *89*, 31–59. https://doi.org/10.1061/JSEDAI.0000430

Yabalak, E. (2018a). Degradation of ticarcillin by subcritical water oxidation method: Application of response surface

methodology and artificial neural network modeling. *Journal of Environmental Science and Health - Part A Toxic/Hazardous Substances and Environmental Engineering*, *53*, 975–985. https://doi.org/10.1080/10934529.2018.1471023

Yabalak, E. (2018b). An approach to apply eco-friendly subcritical water oxidation method in the mineralization of the antibiotic ampicillin. *Journal of Environmental Chemical Engineering*, *6*, 7132–7137. https://doi.org/10.1016/j.jece.2018.10.010

Yabalak, E., Ozay, Y., Gizir, A. M., & Dizge, N. (2021). Water recovery from textile bath wastewater using combined subcritical water oxidation and nanofiltration. *Journal of Cleaner Production*, *290*, 125207. https://doi.org/10.1016/j.jclepro.2020.125207

Yagub, M. T., Sen, T. K., Afroze, S., & Ang, H. M. (2014). Dye and its removal from aqueous solution by adsorption: A review. *Advances in Colloid and Interface Science*, *209*, 172–184. https://doi.org/10.1016/j.cis.2014.04.002

Yalvaç, M., Arslan, H., Saleh, M., Gün, M., & Hekim, M. Ş (2021). Utilizing of bio-adsorbent in zero waste concept: Adsorption study of crystal violet onto the centaurea solstitialis and verbascum thapsus plants. *Pamukkale Üniversitesi Mühendislik Bilimleri Dergisi*, *27*(3), 349–358. https://doi.org/10.5505/pajes.2020.85282

Yao, W., Zhu, W., Wu, Y., Wang, X., & Jianati, T. (2015). Removal of crystal violet dye from wastewater by solidified landfilled sludge and its modified products. *Polish Journal of Environmental Studies*, *24*(2), 777–785.

Yaseen, D. A., & Scholz, M. (2019). Textile dye wastewater characteristics and constituents of synthetic effluents: A critical review. *International Journal of Environmental Science and Technology*, *16*, 1193–1226. https://doi.org/10.1007/s13762-018-2130-z

Yatmaz, H. C., Dizge, N., & Kurt, M. S. (2017). Combination of photocatalytic and membrane distillation hybrid processes for reactive dyes treatment. *Environmental Technology*, *38*, 2743–2751. https://doi.org/10.1080/09593330.2016.1276222